*Kinetics and Catalysis, Vol. 44, No. 2, 2003, pp. 287–296. Translated from Kinetika i Kataliz, Vol. 44, No. 2, 2003, pp. 311–321.*


# Structural Aspect of a Thermal Activation Effect in the $MnO_x/\gamma\text{-}Al_2O_3$ System

**S. V. Tsybulya*, G. N. Kryukova*, T. A. Kriger*, and P. G. Tsyrul'nikov****

** Boreskov Institute of Catalysis, Siberian Division, Russian Academy of Sciences, Novosibirsk, 630090 Russia*

*** Boreskov Institute of Catalysis, Omsk Branch, Siberian Division, Russian Academy of Sciences, Omsk, 644053 Russia*

Received August 6, 2001

**Abstract**—Solid-phase reactions in the aluminum–manganese oxide system, including the structural mechanism of the thermal activation of catalysts, were studied at temperatures up to 1100°C. It was found that the solid-phase reaction at 900–1000°C occurred via two pathways because of the diffusion of manganese ions to aluminum oxide and aluminum ions to manganese oxide. Nanoheterogeneous state of the active component, which was observed in the range 25–600°C, is the product of incomplete decomposition of the high-temperature aluminum–manganese phase $Mn_{2.1-x}Al_{0.9+x}O_4$ ($0 \le x \le 0.6$) with a cubic spinel structure; this phase was equilibrium at the synthesis temperature but metastable below 650°C.

## INTRODUCTION

Manganese–alumina catalysts for deep oxidation are highly active and thermally stable systems whose catalytic properties were described in a number of publications [1–5]. Tsyrul'nikov *et al.* [4] found the effect of the considerable increase in the catalytic activity of the $MnO_x/\gamma\text{-}Al_2O_3$ system after calcination at 900–1000°C. This effect was named the thermal activation effect [6]. It was found that an increase in the activity of a catalyst in oxidation reactions is due to the appearance of a highly dispersed oxide phase formed because of chemical and phase transformations in the system. An active component exhibits a defect structure similar to the structure of the tetragonal $\beta\text{-}Mn_3O_4$ spinel. Simultaneously with the formation of the highly dispersed spinel-like phase, that is, even at 900°C, a phase of $\gamma\text{-}Al_2O_3$ appeared in the system, although this stable modification was formed on the calcination of aluminum oxides at temperatures higher than 1150°C [7].

This unusual phenomenon (the dispersion of an active component over a narrow range of calcination temperatures, the thermal stability of the resulting highly dispersed states, and the formation of $\gamma\text{-}Al_2O_3$ at a temperature much lower than that characteristic of this phase) stimulated us to perform systematic studies of this system: the genesis of its phase composition depending on the preparation procedure and calcination time and the structure, formation conditions, and thermal stability of an active phase.

Previously [8, 9], with the use of electron microscopy and differential dissolution, it was found that aluminum ions (up to 15 at. %) can partially enter into the structure of an active phase as a consequence of the interaction between parent aluminum and magnesium oxides. Tsyrulnikov *et al.* [10] found that a metastable intermediate phase with a cubic spinel structure was formed within the first hours (1 to 2 h) of calcination of the manganese–alumina system. In contrast, Tsybulya *et al.* [11], who studied the behavior of the system at long calcination times, found that, regardless of the preparation procedure, the samples calcined for longer than 20 h exhibited after cooling to room temperature only an $\alpha\text{-}Al_2O_3$ phase and aggregates of nanocrystalline particles 8–10 nm in size (the diffraction pattern of these particles corresponds to the tetragonal $\beta\text{-}Mn_3O_4$ spinel). Finally, Krieger *et al.* [12], who performed a high-temperature X-ray diffraction study of the given system, found that the resulting highly dispersed active phase is the product of incomplete decomposition of a high-temperature cubic manganese–alumina spinel, which is nonequilibrium at room temperature.

Thus, the results of previous studies [8–12] correlated to the equilibrium state diagram of the quasi-binary manganese–alumina system [13] allowed us to consider in detail the overall process of the formation of a manganese–alumina catalyst including the structural aspect of the thermal activation effect. This was the aim of this work.

## EXPERIMENTAL

### *Sample Preparation and Experimental Techniques*

The $MnO_2/\gamma\text{-}Al_2O_3$ (8 and 10% $MnO_2$) samples were prepared by impregnation and mixing techniques in accordance with the published procedure [4]. In the mixing technique, $\gamma\text{-}Al_2O_3$ and $\beta\text{-}MnO_2$ with different dispersity were used as parent oxides. The samples were calcined for 6 h at a particular temperature. Moreover, several sample series were calcined at 970°C for different times that varied from 1 to 24 h.

The X-ray diffraction studies were performed on URD-63 and D-8 diffractometers (Germany) at room

0023-1584/03/4402-0287$25.00 

Phase composition of manganese--alumina catalysts calcined for 6 h at various temperatures

| Phase composition | | | |
|---|---|---|---|
| calcination temperature, °C | impregnation (I) | mixing (II) | mixing (III) |
| 500 | $\gamma$-$Al_2O_3$, $\beta$-$MnO_2$ | $\gamma$-$Al_2O_3$, $\alpha$-$Mn_2O_3$ | – |
| 600 | $\gamma$-$Al_2O_3$, $\alpha$-$Mn_2O_3$ | ″ | $\gamma$-$Al_2O_3$, $\alpha$-$Mn_2O_3$ |
| 700 | ″ | ″ | ″ |
| 800 | ″ | ″ | ″ |
| 900 | $\delta$*- + $\alpha$-$Al_2O_3$ | $\delta$- + $\alpha$-$Al_2O_3$, $\alpha$-$Mn_2O_3$ | $\delta$*- + $\alpha$-$Al_2O_3$, $\alpha$-$Mn_2O_3$, $\beta$-$Mn_3O_4$* |
| 950 | $\delta$*- + $\alpha$-$Al_2O_3$, $\beta$-$Mn_3O_4$* | $\delta$- + $\alpha$-$Al_2O_3$, $\beta$-$Mn_3O_4$ | $\delta$*- + $\alpha$-$Al_2O_3$, $\beta$-$Mn_3O_4$* |
| 1000 | $\alpha$-$Al_2O_3$, $\beta$-$Mn_3O_4$* | $\delta$- + $\alpha$-$Al_2O_3$, $\beta$-$Mn_3O_4$ | $\delta$- + $\alpha$-$Al_2O_3$, $\beta$-$Mn_3O_4$* |
| 1100 | $\alpha$-$Al_2O_3$, $Mn_{1.4}Al_{1.6}O_4$ | $\alpha$-$Al_2O_3$, $\beta$-$Mn_3O_4$, $Mn_{1.4}Al_{1.6}O_4$ | $\alpha$-$Al_2O_3$, $Mn_{1.4}Al_{1.6}O_4$ |

temperature. The high-temperature diffraction experiment was performed on a Siemens D-500 diffractometer with the use of an Anton Paar high-temperature X-ray chamber (Austria). All the diffraction experiments were performed with the use of Cu$K_\alpha$ radiation.

The high-resolution electron-microscopic studies were performed on a JEM-2010 electron microscope (Japan). The X-ray spectrum microanalysis was performed on a CF-200 microscope (the Netherlands) equipped with an EDAX attachment for microanalysis.

## RESULTS

### *Genesis of the Phase Composition*

The table summarizes data on the phase composition of samples calcined at temperatures from 500 to 1100°C. The difference between series II and III, which were prepared using the mixing technique, is that coarsely dispersed $\beta$-$MnO_2$ oxide with a particle size of about 200 nm was used in series II, whereas the particle size of manganese oxide in series III was 30–50 nm (according to TEM data).

Up to a calcination temperature of 900°C, the corresponding manganese oxide and $\gamma$-$Al_2O_3$ phases were present in the samples regardless of the preparation procedure. Changes in the $\gamma$-$Al_2O_3$ lattice parameter did not allow us to draw a reliable conclusion on the dissolution of manganese ions in $\gamma$-$Al_2O_3$ (or the opposite conclusion). However, Kochubei *et al.* [14] noted a change in the IR spectra of $\gamma$-$Al_2O_3$, which was supposedly related to the formation of a solid solution. In any case, if manganese ions are partially dissolved in alumina at calcination temperatures of 500–800°C, the solubility is insignificant or the solid-phase reaction is very slow and is not responsible for the behavior of the system. An active solid-phase reaction began at 900°C (table), and it was especially significant for samples prepared by impregnation [9]. This reaction resulted in the appearance of concentrationally nonuniform [9] solid solutions based on $\delta$-$Al_2O_3$ and $\beta$-$Mn_3O_4$ structures (which are marked with asterisks in the table) and an $\alpha$-$Al_2O_3$ phase as one of the decomposition products of the $\delta$-$Al_2O_3$* solid solution. The sequence of solid-phase reactions in the range of temperatures 900–1000°C, at which the effect of thermal activation of catalysts was observed [4], can be followed in a series of samples calcined at the same temperature but with different calcination times.

Figure 1 demonstrates the X-ray diffraction patterns of samples prepared by impregnation after calcination at 970°C for 1–24 h. An interesting fact is the appearance of a metastable spinel-like cubic phase in the samples calcined for 1 to 2 h (Fig. 1, curve *2*). The lattice parameter $a$ = 8.332(1) Å of this phase and the corresponding chemical composition[1] $Mn_{1.8}Al_{1.2}O_4$ suggest that this phase was formed from manganese oxide as a result of the diffusion of aluminum cations into its structure. The cubic phase observed was not completely ordered (and, consequently, equilibrium): specific extensive defects were detected in its structure by high-resolution electron microscopy (Fig. 2). These defects can be interpreted as the "walls" of cationic vacancies. Previously, defects of this type were detected and studied in nonstoichiometric spinels with a deficiency of bivalent cations, specifically, in the $\gamma$-$Al_2O_3$ oxide prepared by boehmite dehydration [15] and in a low-tem-

[1] Henceforth, the ratio between cations in an aluminum–manganese spinel was determined from a plot of the lattice parameter against the chemical composition of the phase constructed using JCPDS data.

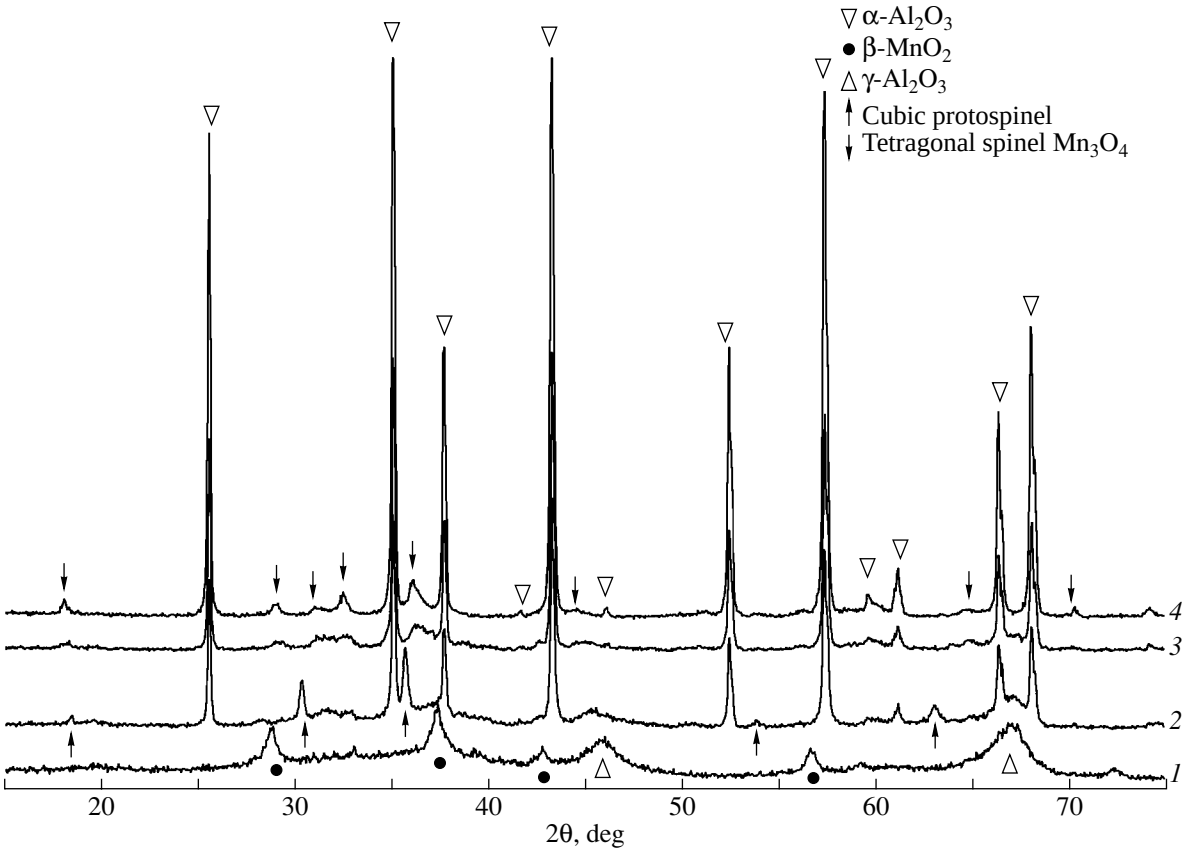


**Fig. 1.** X-ray diffraction patterns of samples calcined at 970°C for (*2*) 2, (*3*) 4, and (*4*) 24 h and (*1*) an initial sample (prepared by impregnation and calcined at 500°C for 6 h).

perature aluminum–magnesium spinel [16]. Thus, based on electron-microscopic data, we can state that the metastable phase observed is cation deficient, and vacancies present in the structure are concentrated as ordered vacancy walls. Note that this intermediate phase with the structure of a defect spinel (protospinel) of the $\gamma$-$Al_2O_3$ type was also detected using EXAFS [14] even at the stage of its formation in a sample calcined at 900°C.

A tetragonal spinel of the $\beta$-$Mn_3O_4$ type, rather than a cubic spinel, appeared in samples calcined for longer than 2 h (Fig. 1, curves *3*, *4*); the diffraction peaks of this spinel were considerably broadened (the size of the coherent-scattering region was ~8 nm). This phase is also a product of the interaction of manganese and aluminum oxides; however, according to differential dissolution data [9], it contains about 10–15 at. % aluminum ions (much lower than the precursor protospinel!). It is interesting that, as the calcination time was further increased, the amount of the tetragonal aluminum–manganese phase gradually increased; however, the dispersity of this phase remained almost unchanged. The final product of the high-temperature synthesis at 970°C was a system that contained only an $\alpha$-$Al_2O_3$ phase and a highly dispersed $\beta$-$Mn_3O_4^*$ phase (this phase was doped with a certain amount of $Al^{3+}$ ions) after cooling. The high dispersity of this phase is noteworthy because neither a further increase in the calcination time (up to 800 h at 950°C [5]) nor an increase in the calcination temperature up to 1100°C [11] resulted in a detectable agglomeration of this phase. We related a dramatic increase in the catalytic activity of test samples to the formation of a nanocrystalline $\beta$-$Mn_3O_4^*$ phase.

Note that, as expected, the calcination of initial samples at temperatures higher than 1000°C resulted in the formation of a well-crystallized cubic aluminum–manganese spinel (table). Thus, at a calcination temperature of 1100°C a spinel with the lattice parameter $a$ = 8.273 (1) Å was formed, which corresponds to the composition $Mn_{1.4}Al_{1.6}O_4$. Thus, the highly dispersed $\beta$-$Mn_3O_4^*$ phase of interest was formed only on the calcination of the aluminum–manganese system in the temperature range 900–1000°C for longer than 3 h.

The genesis of the phase composition of the aluminum–manganese system was discussed in more detail elsewhere [9–11]. In particular, the interactions of manganese and aluminum oxides were considered depending on the sample preparation procedure (impregnation

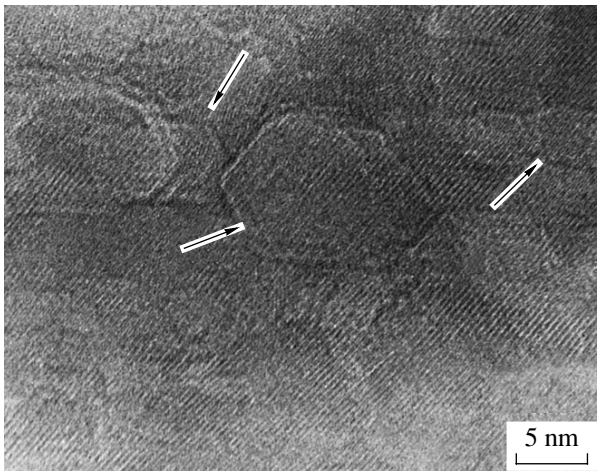


**Fig. 2.** Micrograph of a metastable cubic protospinel particle formed in samples calcined at 970°C for 1 to 2 h. Arrows indicate extensive defects.

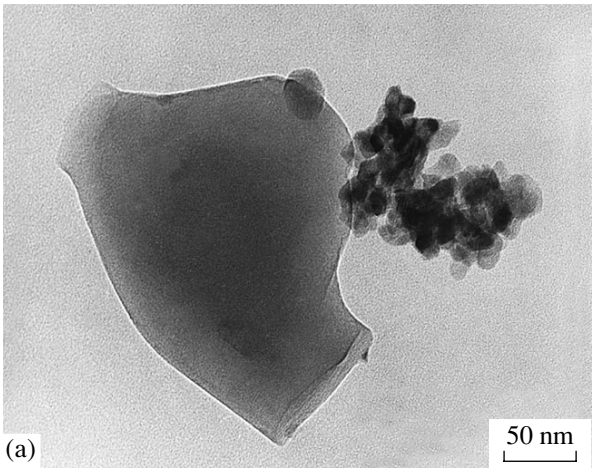


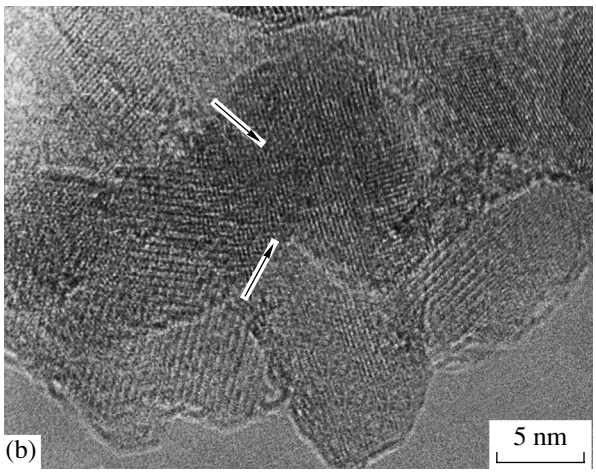


**Fig. 3.** Micrographs of the particles of an aluminum–manganese phase in a sample calcined at 970°C for 24 h: (a) the general view of particle aggregates and (b) a high-resolution micrograph. Arrows indicate regions with a disordered structure.

and mixing with the use of manganese oxides of different dispersity). However, the general conclusion is that $\alpha$-$Al_2O_3$ and $\beta$-$Mn_3O_4$* phases were present in the samples calcined at 900–970°C for longer than 20 h regardless of the preparation procedure. When a coarsely dispersed phase of $\beta$-$MnO_2$ was present as a parent component for mixing, a coarsely dispersed phase of $\beta$-$Mn_3O_4$ was also present in the final product in addition to the above phases (table, series II) as a consequence of the incomplete interaction between manganese and aluminum oxides. In this case, the diffusion of Al ions was limited by the limited surface of the manganese oxide, and the conversion of alumina into the $\alpha$-$Al_2O_3$ phase stimulated by the diffusion of manganese ions into $\delta$-$Al_2O_3$ was complete before the complete conversion of manganese oxide into $\beta$-$Mn_3O_4^*$.

The surprisingly high thermal stability of the highly dispersed state of $\beta$-$Mn_3O_4^*$ and its high catalytic activity stimulated us to perform a detailed study of this phase using electron microscopy.

### *Microstructure of the Active Phase*

Figure 3a demonstrates the micrograph of a sample calcined at 970°C for 24 h. Along with $\alpha$-$Al_2O_3$ particles, coarse (about 100 nm, Fig. 3a) aggregates that consisted of particles 8–10 nm in size, which corresponds to the size of coherent-scattering regions determined in the $\beta$-$Mn_3O_4^*$ phase by X-ray diffraction analysis, were present in the sample. High-resolution micrographs (Fig. 3b) showed that perfect crystalline nanoparticles in the aggregates adjoined regions that exhibited disordered structures and, probably, were X-ray amorphous. The structure of the ordered regions corresponds to the structure of $\beta$-$Mn_3O_4$.

The microanalysis data indicate that the aggregates of particles are highly nonuniform in composition. Along with the regions of manganese oxide doped with 10–15 at % Al ions (which corresponds to the differential dissolution data in [9]) (Fig. 4a), regions with high atomic concentrations of Al ions and with relatively smaller amounts of Mn ions were present in the aggregates (Fig. 4b) (the peaks of Cu in Fig. 4 appeared because the sample was applied to copper gauze; the peak of carbon resulted from the appearance of carbon deposits in the course of measurements).

Keeping in mind that only two phases of $\alpha$-$Al_2O_3$ and $\beta$-$Mn_3O_4^*$ were detected from X-ray diffraction, the set of data obtained by high-resolution electron microscopy and microanalysis allowed us to conclude that the crystalline particles in the aggregates are the particles of the $\beta$-$Mn_3O_4$ oxide doped with a small amount of aluminum ions. At the same time, aluminum ions were predominant in disordered regions.

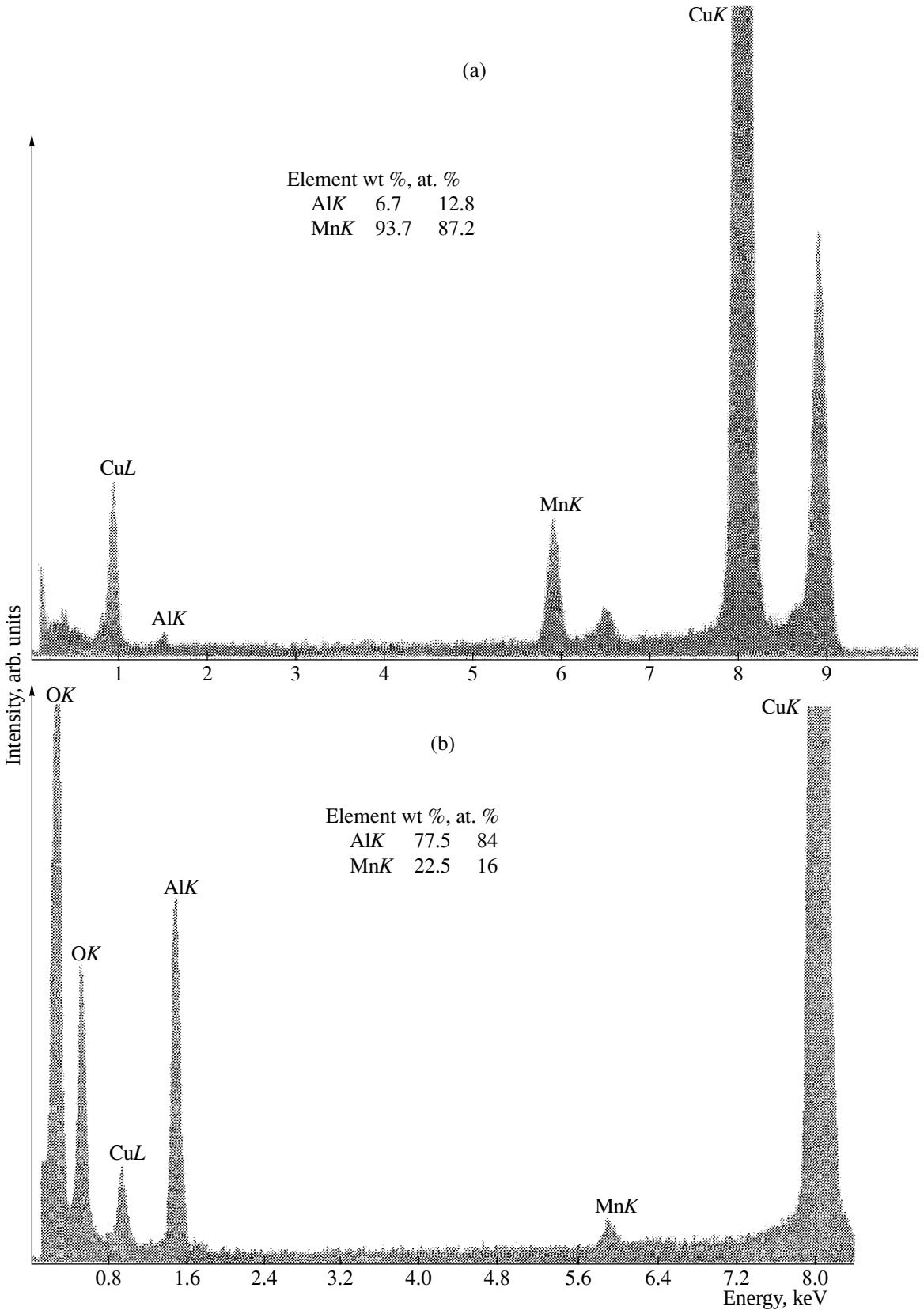


**Fig. 4.** X-ray spectrum microanalysis data for different regions of manganese–alumina particle aggregates: (a) a crystalline block and (b) a region with a disordered structure (Fig. 3). Cu*L*, Mn*L*, Al*K*, Cu*K*, O*K*, C*K*—are spectral lines of the characteristic X-ray irradiation of *K* and *L* series for Cu, Mn, O, and C, respectively.

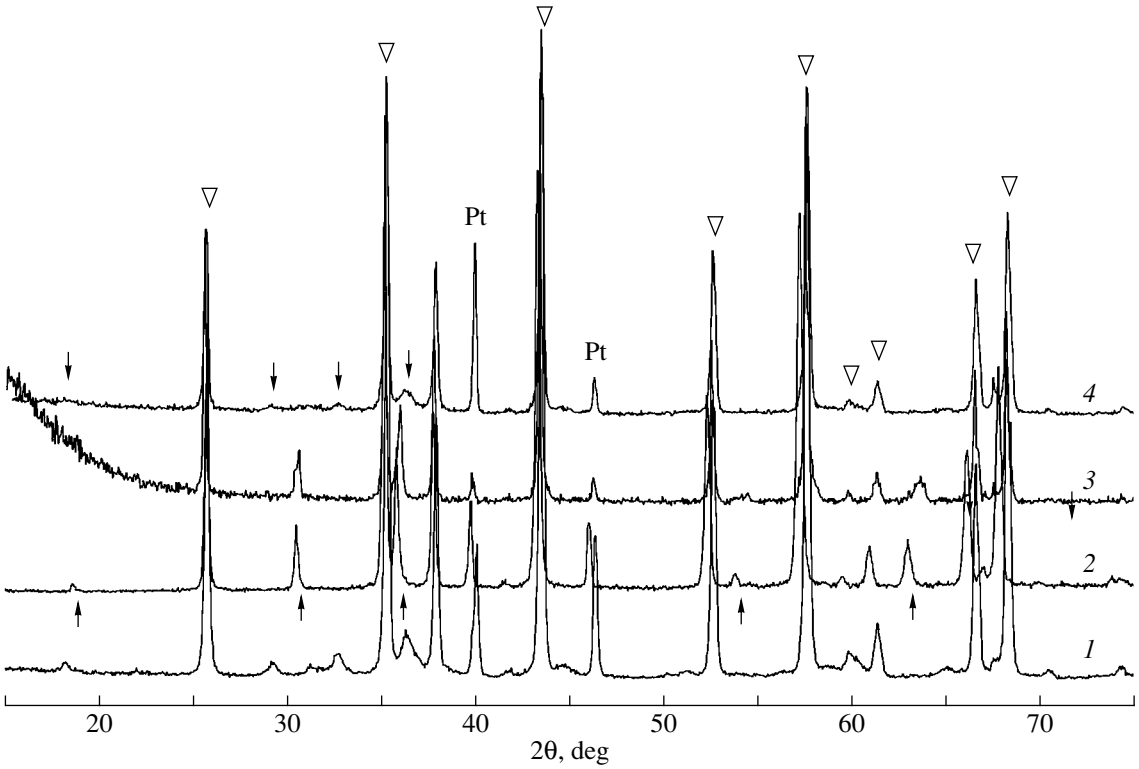


**Fig. 5.** X-ray diffraction patterns of a catalyst measured in the high-temperature chamber: (*1*) starting sample, (*2*) after heating to 950°C, (*3*) after rapidly cooling (quenched sample), and (*4*) after slowly cooling (↑ cubic spinel; ↓ tetragonal spinel β-$Mn_3O_4^*$; ∇ α-$Al_2O_3$; and Pt, diffraction peaks from the platinum heater of the high-temperature chamber).

It is evident that the detected aggregates of nanoparticles occur in a nonequilibrium (metastable) state, which will hardly be formed and retained for a long calcination time directly in the course of a high-temperature (equilibrium) synthesis. More likely, the observed nanoheterogeneous state would be expected to result from partial degradation of a high-temperature phase, which is equilibrium at the synthesis temperature, in the course of cooling it to room temperature. This hypothesis could be tested by performing a diffraction experiment with the use of a high-temperature X-ray chamber.

*Results of a High-Temperature Diffraction Study*

To perform the high-temperature diffraction experiment, a sample calcined in a muffle furnace at 970°C for 24 h was taken as the starting sample. This sample (Fig. 5, curve *1*) was a system whose constituents were α-$Al_2O_3$ and the above nanoheterogeneous state designated as β-$Mn_3O_4^*$, because the diffraction pattern of this phase generally corresponds to the diffraction pattern of a β-$Mn_3O_4$ tetragonal spinel.

The sample was heated in a high-temperature X-ray chamber to 950°C at a rate of 10 K/min. After the heating, the diffraction pattern of the test sample dramatically changed (Fig. 5, curve *2*). Peaks due to the highly dispersed tetragonal phase were absent from this diffraction pattern. At the same time, along with the diffraction peaks of α-$Al_2O_3$, narrow diffraction peaks were observed, which correspond to the cubic spinel structure. Thus, the tetragonal spinel–cubic spinel phase transition and a change (recrystallization) in the sample nanostructure occurred on heating.

The behavior of the system on cooling was found to crucially depend upon the conditions of cooling. The cooling was performed as follows: (1) rapid cooling by switching off the heat source after attaining a temperature of 950°C or (2) slow cooling by decreasing the temperature at a rate of 10 K/min when diffraction patterns were recorded at regular intervals of 50°C.

Figure 5 (curve *3*) demonstrates the X-ray diffraction pattern of a sample cooled to room temperature by rapid cooling. It is almost identical to the diffraction pattern measured at 950°C; that is, it is mainly characterized by the presence of diffraction peaks that correspond to the cubic spinel phase. The electron-microscopic data for a quenched sample indicate that this phase is well-ordered, and only some structural microdistortions were observed, which probably appeared in the course of cooling. The lattice parameter $a$ = 8.287(1) Å corresponds to the composition $Mn_{1.5}Al_{1.5}O_4$.

Thus, we found that the high-temperature cubic phase is easy to quench. At the same time, it is metastable at room temperature, as found upon slowly cooling the sample. This mode of cooling resulted in the transition from a well-crystallized cubic phase to a highly dispersed tetragonal phase (Fig. 5, curve *4*), whose diffraction pattern substantially corresponds to the diffraction pattern of the parent sample. Both the tetragonal spinel–cubic spinel transition and the nanostructured organization of the aluminum–manganese phase are reversible. Note that the mode of gradually cooling corresponds largely to the conditions of slow cooling in a muffle furnace; because of this, the nanocrystalline state of the active component is also formed in the synthesis of catalysts.

Figure 6 illustrates the sequence of phase transitions in the course of sample heating and cooling. It can be seen that the disappearance of the diffraction peaks of the tetragonal phase and the appearance of those of the cubic phase (as well as the reverse process) occurred slowly. In this case, the temperature ranges of the coexistence of both phases were detected. Thus, in the course of heating, the cubic phase appeared even at 650°C, whereas the tetragonal phase completely disappeared only at 800°C. On cooling, the tetragonal phase was detected at 650°C, whereas the peaks of the cubic phase completely disappeared at 500°C.

At the instant of changing to a cubic structure at 650°C, the aluminum–manganese phase had the lattice parameter $a = 8.387(2)$ Å (with consideration for the coefficient of thermal expansion) and, correspondingly, the composition $Mn_{2.1}Al_{0.9}O_4$, whereas it was noted above that the composition at 950°C was $Mn_{1.5}Al_{1.5}O_4$. These data unambiguously suggest that the diffusion of aluminum ions into the bulk of the spinel structure takes place (simultaneously with structure perfection; Fig. 5, curve *2*). The reverse process of decomposition of the resulting solid solution takes place on cooling.

Thus, the tested active aluminum–manganese phase, which is a nanoheterogeneous system, is the product of partial decomposition of the solid solution $Mn_{3-x}Al_xO_4$ ($x \le 1.5$), which was equilibrium at the synthesis temperature but became metastable as the temperature decreased. This solid solution underwent a phase transition at $x < 0.9$ (the composition with $x = 0.9$ was in equilibrium at ~650°C).

The reversible high-temperature tetragonal spinel–cubic spinel phase transition is well known for both the $\beta$-$Mn_3O_4$ phase [17] and $Mn_{3-x}Al_xO_4$ solid solutions at $0.2 \le x < 0.9$ [13]. The cooperative Jahn–Teller effect (the spatially synchronized lowering of the symmetry of coordination polyhedrons in which transition metal cations in orbitally degenerated states occur [18]) is responsible for the nature of this transition. The $Mn^{3+}$ ion in an octahedral coordination belongs to these cations, which give rise to a structural phase transition accompanied by the deformation of the entire crystal. Therefore, the phase transition itself is regular at a sufficiently high concentration of $Mn^{3+}$ cations. However, the fact that the solid solutions $Mn_{3-x}Al_xO_4$ with $0.9 \le x \le 1.5$ undergo decomposition on cooling and the structure of the resulting nanocrystalline state are of interest. Evidently, the metastable character of the test solid solutions is associated with the fact that $Mn^{3+}$ ions are prone to clustering in spinel structures [19], which results in the displacement of aluminum ions with increasing temperature.

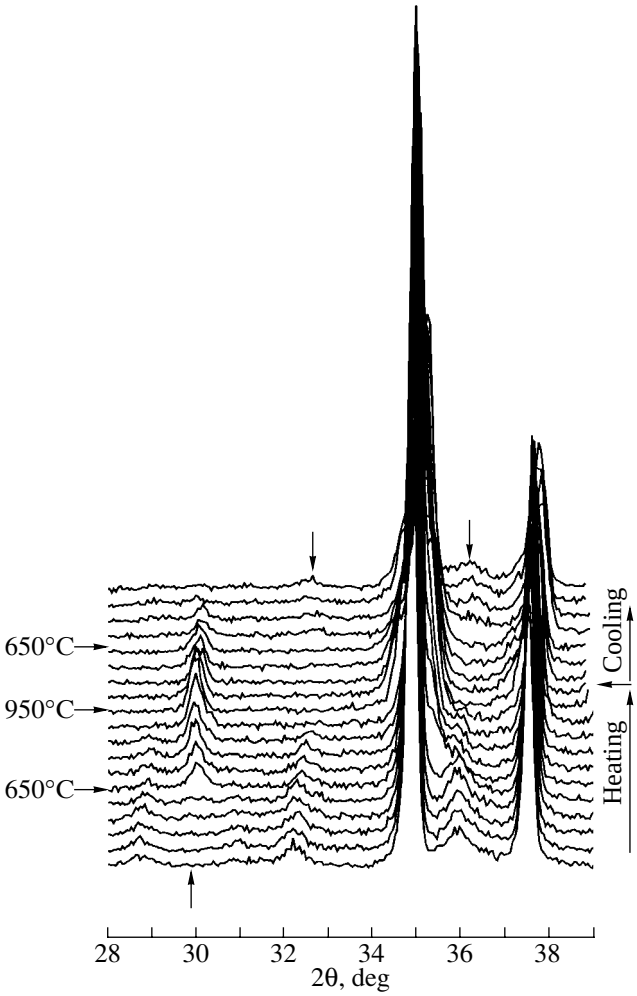


**Fig. 6.** Phase transformations in the aluminum–manganese system on heating and cooling in the high-temperature X-ray chamber (↑ cubic spinel and ↓ tetragonal spinel $\beta$-$Mn_3O_4^*$).

## DISCUSSION

It is reasonable to discuss the experimental data on the formation of the phase composition of manganese–alumina catalysts, which are mainly associated with nonequilibrium kinetically mediated factors, together with data on the equilibrium state diagram of the quasi-binary aluminum–manganese system (Fig. 7).

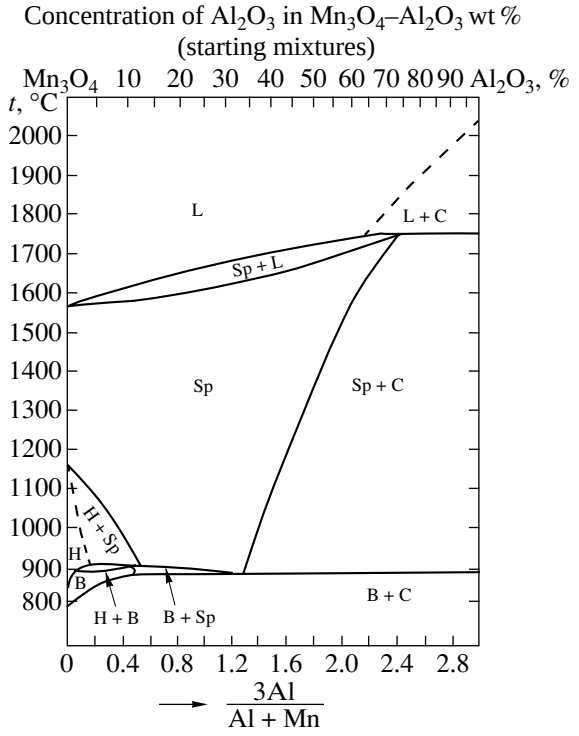


**Fig. 7.** Phase diagram of the quasi-binary aluminum–manganese system [13]: H is hausmannite β-$Mn_3O_4$, C is corundum α-$Al_2O_3$, B is a solid solution based on the α-$Mn_2O_3$ structure, Sp is aluminum–manganese spinel, and L is a liquid melt.

Data on the equilibrium states of the system at different ratios of alumina and manganese oxide in many respects explain the processes that occur in the system. First, note that the diffusion of Al cations into manganese oxide practically did not occur at temperatures lower than 900°C. It is likely that under the conditions of our experiments the diffusion of manganese ions into metastable aluminum oxide was also highly insignificant. The active interaction of the oxides at temperatures higher than 900°C may be associated with two factors. First, it is well known that in this temperature region both of the oxides undergo transformations (α-$Mn_2O_3$ into β-$Mn_3O_4$ and γ-$Al_2O_3$ into δ-$Al_2O_3$), which dramatically increased their reactivity toward solid-phase reactions. Second, after the conversion of α-$Mn_2O_3$ into β-$Mn_3O_4$, the structures of both of the oxides became closely related (spinel-like), and there is no doubt that the affinity between the structures is also favorable for the interaction between two phases. Thus, the active diffusion of both aluminum ions into manganese oxide and manganese ions into alumina began at temperatures above 900°C.

It follows from the phase diagram (Fig. 7) that, in the compositions with an excess of aluminum, two phases occur in an equilibrium: α-$Al_2O_3$ and an aluminum–manganese spinel with a limiting composition with respect to the content of aluminum ions (this is approximately $Mn_{1.5}Al_{1.5}O_4$ at a temperature of 950°C; note that the spinel phase in a sample quenched by rapid cooling exhibited the same composition). Therefore, the diffusion of manganese ions into the metastable phase of alumina (in this case, this is a transient sate of γ- to δ-$Al_2O_3$) destabilized the structure of the latter and facilitated the decomposition of the resulting nonequilibrium solid solution into two equilibrium phases at a given temperature. This explains the appearance of an α-$Al_2O_3$ phase at temperatures much lower than ordinary values. The fact that the addition of the β-$MnO_2$ manganese oxide even in an amount of ~5 wt % facilitates the earlier transition of low-temperature aluminum oxides to α-$Al_2O_3$ was also supported by published data [20]. Thus, the first solid-phase reaction path depends on the diffusion of manganese ions to the metastable form of alumina followed by the decomposition of the resulting nonequilibrium solid solution.

The second solid-phase reaction path, the diffusion of aluminum ions to manganese oxide, resulted in the formation of a metastable cation-deficient spinel at the first stage. The appearance of a metastable cubic spinel (protospinel) upon calcination for 1 to 2 h was not directly related to the effects of dispersion and thermal activation of manganese–alumina catalysts, which are analyzed in this work. However, this is an interesting fact, which should be discussed separately. It is believed that this intermediate phase is formed because of the simultaneous occurrence of two processes in the system at a given temperature: (1) the chemical conversion of the precursor α-$Mn_2O_3$ phase into β-$Mn_3O_4$ and (2) the diffusion of Al ions into the structure of this phase. The former is associated with the loss of oxygen and the partial reduction of $Mn^{3+}$ to $Mn^{2+}$, and it was accompanied by a structural rearrangement—transition from the bixbyite structure type to the spinel structure type. Based on X-ray and electron diffraction data, it is clear that the structure of the tested active phase generally corresponds to the spinel structure; correspondingly, the anions form the closest cubic packing, which is characteristic of spinels. However, it is likely that this phase was deficient in $Mn^{2+}$ cations at this stage of the reaction, taking into account the diffusion of trivalent $Al^{3+}$ cations. Therefore, to provide electric neutrality, this phase should be cation deficient (similarly to γ-$Al_2O_3$) and low-temperature nonstoichiometric aluminum–magnesium (proto)spinel [15, 16], whose stoichiometry is due to extensive defects. The fact that the concentration of $Mn^{2+}$ ions increased gradually and slowly (simultaneously with a decrease in the concentration of $Mn^{3+}$) was supported by diffuse-reflectance electronic spectroscopy [14]. According to these data, in a series of samples calcined at various temperatures for 6 h, the appearance of an absorption band that corresponds to $Mn^{2+}$ was observed only in a sample calcined at 1000°C. The intensity of this band continued to increase with calcination temperature.

The metastable aluminum–manganese protospinel phase detected (as distinct from an equilibrium solid

solution at 950°C) remained cubic on cooling. It is well known [16] that, in the presence of the above extensive defects, a portion of cations occur at positions that are uncharacteristic of spinel; in our case, this was supported by EXAFS data [14]. It is likely that this state is sufficiently stable; probably, it prevents the clustering of Jahn–Teller cations and the displacement of Al ions. That is, defects of this type stabilize the composition and structure of the protospinel phase at room temperature.

The oxidation state of manganese ions gradually decreased with calcination time; this resulted in the formation of stoichiometric (in terms of the absence of cationic vacancies) aluminum–manganese spinel. That is, finally, the diffusion of aluminum ions to manganese oxide also resulted in the formation of cubic (at the synthesis temperature) spinel with a limiting aluminum content ($x \sim 1.5$) at the given temperature, as well as the diffusion of manganese ions to alumina, although the mechanisms of formation of equilibrium spinel are dramatically different in these cases.

Thus, the following two solid-phase reaction pathways take place in the aluminum–manganese system:

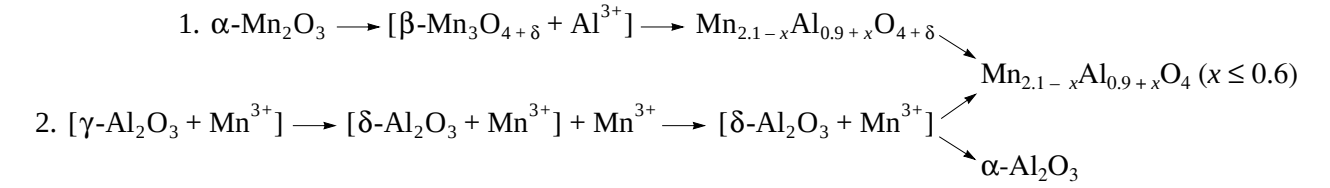


The final product of this high-temperature synthesis is a system of $\alpha$-$Al_2O_3$ and a cubic spinel, which was equilibrium at a given temperature but decomposed on slowly cooling.

The cubic structure was retained up to the composition $Mn_{2.1}Al_{0.9}O_4$, which was detected at 650°C, whereas a further relative increase in the concentration of the $Mn^{3+}$ cation induced the transition to a tetragonal phase. However, the decomposition of the solid solution also continued after the phase transition because the finally formed nanocrystalline $\beta$-$Mn_3O_4$ particles contained no more than 15 at % Al ions according to the above microanalysis data and published data [9] on differential dissolution.

We emphasize that the operation temperature of manganese–alumina catalysts is usually no higher than 600°C, which is much lower than the temperature of high-temperature synthesis. In this case, the aluminum–manganese phase retained its highly dispersed nanoheterogeneous state, which may be responsible for its high catalytic activity.

The occurrence of the two solid-phase reaction pathways is an important circumstance because it allowed us to indicate approaches to the target-oriented control of the phase composition and the structure of manganese–alumina catalysts using a kinetic factor. Indeed, we can attempt to slow down or accelerate one of the reaction pathways by varying the phase composition and dispersity of starting reagents or the calcination temperature or by using chemical additives; this will result in a predictable change in the final product. Thus, for example, it was mentioned above that with the use of parent manganese oxide with a low surface area the first solid-phase reaction pathway (the diffusion of Al ions to manganese oxide) was dramatically slowed down, and alumina was converted into the $\alpha$-phase before manganese oxide completely managed to be converted into an aluminum–manganese spinel. An increase in the calcination temperature accelerated the transition to $\alpha$-$Al_2O_3$; in this case, the appearance of spinels with higher concentrations of manganese ions would be expected. In contrast, rare-earth oxide additives stabilized the low-temperature forms of aluminum oxide [20]. It is likely that, because of this, an active aluminum–manganese phase can be formed with the retention of the high surface area of the support. The phase composition of the parent aluminum oxide can also play a controlling role. Thus, Tsikoza *et al.* [20] found that the addition of up to 15% $\chi$-$Al_2O_3$ to $\gamma$-$Al_2O_3$ noticeably increased the degree of the interaction of manganese and aluminum oxides at temperatures lower than 900°C; this finally resulted in the intensification of the thermal activation effect.

## CONCLUSION

The studies of phase transitions in the aluminum–manganese oxide system allowed us to consider in detail the formation and structure of an active phase. In the course of a solid-phase reaction between manganese and aluminum oxides at 900–1000°C, the following intermediate phases are formed at the initial stage (1- to 2-h calcination): a solid solution of manganese ions in aluminum oxide and an aluminum–manganese phase of the protospinel type, which is formed because of the incomplete conversion of $\alpha$-$Mn_2O_3$ into $\beta$-$Mn_3O_4$ and the diffusion of aluminum ions into its structure. Equilibrium solid solutions with a spinel structure $Mn_{3-x}Al_xO_4$ (to $x \sim 1.5$) are formed upon calcination for a longer time; however, they decompose on cooling. The cooperative Jahn–Teller effect is responsible for the decomposition, which results in the formation of a nanoheterogeneous state. The structure of this state exhibits nanosized crystallites enriched in $Mn^{3+}$ ions

and disordered intercrystalline regions enriched in aluminum ions. At the reaction temperatures, the aluminum–manganese phase is a nanoheterogeneous system under conditions of an unstable equilibrium, which may be responsible for its high catalytic activity.

## ACKNOWLEDGMENTS

This work was supported by the Russian Foundation for Basic Research (project no. 99-03-32135a).

## REFERENCES

1. Kiknadze, L.P. and Cherenkov, G.V., *Geterogennye kataliticheskie protsessy* (Heterogeneous Catalytic Processes), Leningrad: Leningrad Gos. Univ., 1979, p. 52.
2. Vlasenko, V.M. and Mal'chenko, L.A., *Teor. Eksp. Khim.*, 1984, vol. 20, p. 49.
3. Baltanas, M.A., Stilles, A.B., and Katzer, J.R., *Appl. Catal.*, 1986, vol. 20, no. 15, p. 31.
4. Tsyrul'nikov, P.G., Sal'nikov, V.A., Drozdov, V.A., Shtuken, S.A., Bubnov, A.V., Grigorov, E.I., Kalinkin, A.V., and Zaikovskii, V.I., *Kinet. Katal.*, 1991, vol. 32, p. 439.
5. Tsyrulnikov, P.G., Kovalenko, O.N., Gogin, L.L., Starostina, T.G., Noskov, A.S., Kalinkin, A.V., Kryukova, G.N., Tsybulya, S.V., Kudrja, E.N., and Bubnov, A.V., *Appl. Catal., A*, 1998, vol. 167, p. 31.
6. Tsyrul'nikov, P.G., *Doctoral (Chem.) Dissertation*, Novosibirsk, 1997.
7. Ivanova, A.S., Litvak, G.S., Kryukova, G.N., Tsybulya, S., and Paukshtis, E.A., *Kinet. Katal.*, 2000, vol. 41, p. 137.
8. Kryukova, G.N., *Abstracts of Papers*, Arizona Int. School, 1996, p. 16.
9. Tsybulya, S.V., Kryukova, G.N., Vlasov, A.A., Boldyreva, N.N., Kovalenko, O.N., and Tsyrul'nikov, P.G., *React. Kinet. Catal. Lett.*, 1998, vol. 64, no. 1, p. 113.
10. Tsyrulnikov, P.G., Tsybulya, S.V., Kryukova, G.N., Boronin, A.I., Starostina, T.G., Bubnov, A.V., and Kudrya, E.N., *J. Mol. Catal., A: Chem.*, 2002, vol. 179, p. 213.
11. Tsybulya, S.V., Kryukova, G.N., and Kovalenko, O.N., *Mater. Struct. Chem., Biol. Phys. Technol. A*, 1998, vol. 5, p. 47.
12. Krieger, T.A., Tsybulya, S.V., and Tsyrulnikov, R.G., *React. Kinet. Catal. Lett.*, 2002, vol. 75, no. 1, p. 141.
13. Dekker, E.H.L.J. and Rieck, G.D., *Z. Anorg. Allg. Chem.*, 1975, vol. 415, p. 68.
14. Kochubei, D.I., Kriventsov, V.V., Kustova, G.N., Odegova, G.V., Tsyrul'nikov, P.G., and Kudrya, E.N., *Kinet. Katal.*, 1998, vol. 39, no. 2, p. 294.
15. Kryukova, G.N., Klenov, D.O., Ivanova, A.S., and Tsybulya, S.V., *J. Europ. Ceram. Soc.*, 2000, vol. 20, p. 1187.
16. Tsybulya, S.V., Solov'eva, L.P., Kryukova, G.N., and Moroz, E.M., *Zh. Strukt. Khim.*, 1991, vol. 32, no. 2, p. 18.
17. Pollert, E., *J. Solid State Chem.*, 1980, vol. 33, p. 305.
18. Krupicka, S., *Physik der Ferrite und der Verwandten Magnetischen Oxide*, Praga: Academia, 1973, vol. 1.
19. Balakirev, V.F., Barkhatov, V.P., Golikov, Yu.V., and Maizel', S.G., *Manganity: ravnovesnye i nestabil'nye sostoyaniya*, Yekaterinburg: Inst. Metallurg., 2000.
20. Tsikoza, L.T., Ismagilov, Z.R., Shkrabina, R.A., Koryabkina, N.A., Ushakov, V.A., Kuznetsov, V.V., and Ovsyannikova, I.A., *Mater. seminara pamyati prof. V.V. Popovskogo "Zakonomernosti glubokogo okisleniya veshchestv na tverdykh katalizatorakh"* (Proc. Popovskii Memorial Seminar on the Regularities of Deep Oxidation of Substances on Solid Catalysts), Novosibirsk, 2000, p. 276.